  Bull. Chem. Soc. Jpn., 62, 1421—1431 (1989)

Studies of Liquid Water by Computer Simulations. VI. Transport Properties of Carravetta-Clementi Water

Yosuke KATAOKA
Department of Chemistry, Faculty of Science, Kyoto University, Kyoto 606
(Received October 24, 1988)

The micro canonical molecular dynamics simulations of liquid water were performed at different temperatures and densities in order to investigate the anomalies of the transport coefficients. The nonempirical Carravetta-Clementi potential was used for the system with 216 molecules in a cubic cell. The order of magnitude of the nonempirically calculated self-diffusion coefficient, shear viscosity, bulk viscosity, and thermal conductivity were in agreement with experimental results. These transport properties were recognized as anomalous as in real liquid water. The temperature-dependence of these quantities was in agreement with the observed values under pressure of 50 MPa. The effects of compression on these transport coefficients were reproduced qualitatively. The obtained bulk viscosity was larger than the shear viscosity at low temperatures in accordance with experiments. The contribution of rotational motion to thermal conductivity seems to be responsible for the anomalous temperature-dependence of thermal conductivity. Several decay constants of the time correlation functions were obtained. The frequency spectra of the correlation functions were discussed. No marked molecule number dependence was observed in the calculated transport coefficients of Matsuoka-Clementi-Yoshimine water.

We have carried out the molecular dynamics (MD) simulation to study the effect of density and temperature on the transport properties of liquid water. This problem was examined in the fourth paper[1] of this series by a simplified 2-dimensional water-like model.[2,3] Although most of the transport properties were reproduced qualitatively, the maximum of thermal conductivity as a function of temperature was not verified.[1]

In the preceding paper[4] we showed that the anomalous thermodynamic properties observed experimentally are nonempirically reproduced on a semi-quantitative level with Carravetta-Clementi (CC) potential.[5] Our study on the liquid-vapor interface of CC water gave reasonable thermodynamic properties.[6] For these reasons we will report in the present paper on MD simulations with CC potential to examine the transport properties of liquid water.

The most interesting characteristics of the transport properties of liquid water are summarized as follows:[7] The initial application of pressure decreases the viscosity and increases the self-diffusion coefficient below about 300 K. The thermal conductivity of liquid water has a maximum as a function of temperature under a constant pressure. Although the density dependence of the self-diffusion coefficient was already studied by MD,[8–14] it seems that the viscosity and the thermal conductivity of liquid water have been studied only at normal conditions (at room temperature and volume, $V=18\ \mathrm{cm^3\ mol^{-1}}$).[13] Therefore, we are going to perform MD simulations at different temperatures and densities. Transport coefficients were calculated by the standard Kubo formula.[15–17]

The dynamical properties of liquid water were studied by Matsuoka-Clementi-Yoshimine (MCY) potential[18] at several state points by Impey et al.[9] They showed that the main features of spectroscopic and transport properties of real water are interpreted by their MD simulations, although some spectra are not reproduced. The collective dynamics in MCY and three body water was studied by Wojcik and Clementi.[13] The calculated shear viscosity is well compared with the experimental value at room temperature and normal density. For this reason, MCY potential is one of the most promising models in the study of transport properties of liquid water. We will further survey the fluid state over a wide range of temperature and density. For such purpose, CC potential is more convenient than MCY model, because the equation of state of CC water has been given by us.[4]

In the fourth paper of this series,[1] we used the constant temperature-pressure MD,[19,20] because this method is more convenient to obtain temperature dependence or pressure dependence of the system. We found, however, that the bulk viscosity obtained by the constant pressure MD is wrong.[1] The value of the shear viscosity calculated by constant temperature-pressure MD seemed to scatter more than that by the micro canonical MD.[1] For this reason the micro canonical MD method is used in this paper.

The molecule number dependence of the transport coefficients was examined with MCY water.[18] The transport coefficients of the systems with 216 and 1000 molecules were compared with the Wojcik and Clementi's result on a 512-molecule system.[13]

The contribution of rotational motion to thermal conductivity is calculated in order to examine the origin of the anomalous temperature dependence. The decaying and oscillatory characters of the time correlation functions related to the transport coefficients are analyzed and compared with those of simple liquids.[21–29]

Molecular Dynamics Calculations

The molecular dynamics method is essentially the same as the previous one.[4] The program MDMPOL coded by Smith and Fincham[30] is used as the basis of the present program. The program calculates the time evolution of the system using a leapfrog algorithm for the center of mass motion and a leapfrog-quaternion algorithm for the angular motion. The electrostatic forces and energy were calculated by the Ewald method. The short range terms were cut off at half of the MD cell width for the 216-molecule system. When the system has 1000 molecules, the cutoff distance is the same as that of the 216-molecule system of the same number density. The cpu time was 0.23 and 1.3 s/step for 216- and 1000-molecule systems respectively by FACOM VP-400E vector processor at Kyoto University Data Processing Center, which includes the calculations of stress tensor components and heat currents.

The time step in this work was 0.5 fs. The root mean square fluctuation of the total energy was less than 0.02% in the case of 40000-step run. The initial data at each state were those of the aged state obtained by the previous calculations.[4] The 18000-, 24000-, or 40000-step runs were repeated several times, from which the molecular dynamics statistical averages were obtained.

The self-diffusion coefficient D was calculated from the mean square displacement $<\Delta r^2>$ and the velocity auto-correlation function given below:[31]

$$D = \lim_{t\to\infty} \frac{<\Delta r^2>}{6t} \tag{1}$$

and

$$D = \frac{1}{3}\int_0^\infty <v(t)\cdot v(0)>\mathrm{d}t. \tag{2}$$

The shear viscosity η_S and the bulk viscosity η_B were calculated by the standard Kubo type formula:[15–17]

$$\eta_s = \frac{1}{\kappa_B TV}\int_0^\infty <J^{xy}(t)J^{xy}(0)>\mathrm{d}t, \tag{3}$$

$$\eta_B = \frac{1}{9\kappa_B TV}\sum_{\substack{\alpha=x,y,z\\ \beta=x,y,z}}\int_0^\infty <[J^{\alpha\alpha}(t) - <J^{\alpha\alpha}>]\cdot[J^{\beta\beta}(0) - <J^{\beta\beta}>]>\mathrm{d}t, \tag{4}$$

$$J^{\alpha\beta} = M\sum_{i=1}^{N} v_{i\alpha}v_{i\beta} + \sum_{i=1}^{N} r_{i\alpha}f_{i\beta}, \tag{5}$$

where M is the mass of the molecule, v_i the velocity of the i-th molecule, r_i means the position of the i-th molecule, and f_i is the force that the i-th molecule feels. The suffix α means the α-component of the vector. The Boltzmann constant, temperature, volume, and number of molecules in the basic cell are written as κ_B, T, V, and N, respectively.

The thermal conductivity λ was calculated by the correlation function of the heat current $S(t)$:[15–17]

$$\lambda = \frac{1}{3\kappa_B T^2 V}\int_0^\infty <S(t)\cdot S(0)>\mathrm{d}t \tag{6}$$

and

$$S(t) = \frac{\mathrm{d}}{\mathrm{d}t}\sum_{i=1}^{N} H_i r_i, \tag{7}$$

where H_i is the contribution of the i-th molecule to the total Hamiltonian of the system $\mathscr{H}$:

$$\mathscr{H} = \sum_{i=1}^{N} H_i$$

and

$$H_i = K_{\mathrm{TRANS}}(i) + K_{\mathrm{ROT}}(i) + \frac{1}{2}\sum_{j=1}^{N} U_{ij}, \tag{8}$$

where $K(i)$ is the kinetic energy and U_{ij} is the molecular interaction energy between molecule i and j.

The representative range of the time integration of the correlation function is $0 \leqq t \leqq 1$ ps. The averages of at least 14000 values were taken for the initial time. An example of convergence characteristics is shown in Fig. 1 for shear viscosity. It is seen that the cumulative average is stable although the partial average scatters.

Molecule Number Dependence

As the first step, we are going to see whether 216 molecules are enough for the calculation of transport coefficients. For this purpose, the coefficients of the 216-, 512-, and 1000-molecule system are compared with each other. Wojcik and Clementi[13] gave the results on the 512-molecule system with MCY potential[18] at normal conditions. The systems with 216 and 1000 MCY molecules are compared with their results

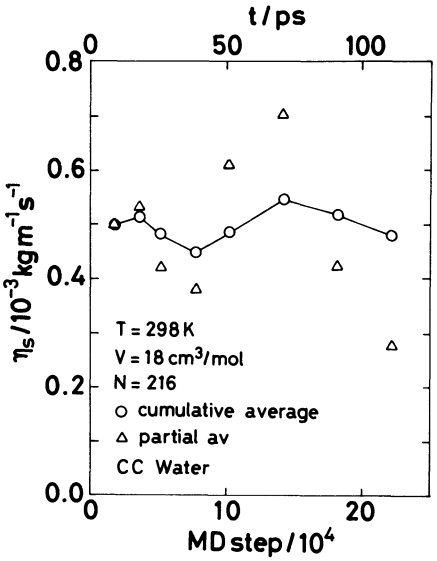

Fig. 1. Convergence characteristics of the shear viscosity.

Table 1. Molecule Number Dependence of the Properties of MCY Water, N=512 case is given by Wojcik and Clementi[13]

		MCY water		CC water	obs
N	1000	512	216	216	obs
T/K	300±2	296	295±1	298±1	298
V cm^3 mol^{-1}	18	18.018	18	18	18.050
P/MPa	829±7	843	832±12	248±8	20
U/kJ mol^{-1}	−28.23±0.06	−28.3	−28.46±0.05	−31.5±0.05	−33.9
G_K	1.6		1.5	1.9	4.1
D/10^{-9} m^2 s^{-1}	2.9 ±0.1		2.4 ±0.3	3.9±0.3	2.85
η_s/10^{-3} kg ms^{-1}	0.4 ±0.2	0.6	0.6 ±0.1	0.5±0.1	0.9
η_B/10^{-3} kg ms^{-1}	0.8 ±0.2	0.8	1.1 ±0.4	0.9±0.4	1.2
l/W mK^{-1}	1.6 ±0.3	1.35	1.3 ±0.3	1.1±0.3	0.59

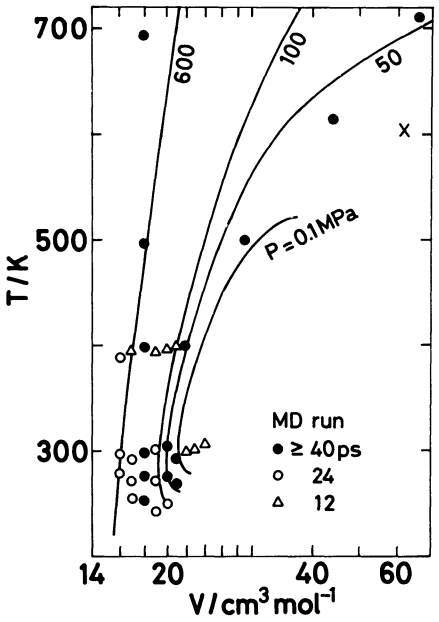

Fig. 2. Map of simulated state points. The G-type equation of sate[4] is drawn by solid lines. The symbol cross means the critical point in the G-type equation of state.

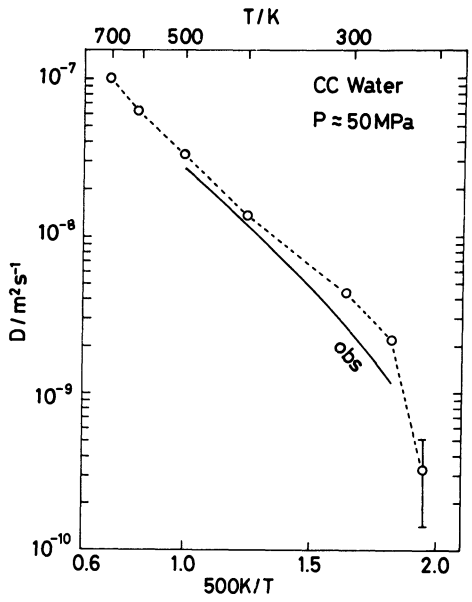

Fig. 3. The self-diffusion coefficient D is plotted against 500 K/T, where pressure P is about 50 MPa. The experimental results at P=50 MPa are shown by the solid line.[35-39]

in Table 1. No marked molecule number dependence is seen in this table. Hence, the basic cell with 216 molecules has been employed hereafter because of simplicity.

Table 1 also includes the coefficients of CC water. They are not so different from those of MCY water. As we have obtained the equation of state (EOS)[4] for CC model, we use CC potential[5] hereafter.

The values of Kirkwood orientational correlation factor G_K are also given, although they are preliminary; it is known that very long MD run is needed to evaluate this quantity.[32-34] These are obtained as follows:

$$G_K = <(\sum_{i=1}^{N} \mu_i)^2>/N, \quad (9)$$

where μ_i is the unit vector along the dipole direction of molecule i. The obtained values of G_K for MCY and CC water were small compared with the experimental values.[32] A similar result on MCY water was given by Neumann.[32]

Temperature and Volume Dependence

In this section, the calculated transport coefficients are compared with the experimental results. We carried out many MD simulations of the 216-molecule system with CC potential[5] in order to examine the temperature and density dependence of the transport coefficients as shown in Fig. 2. Some state points correspond to the states with pressure P of about 50 MPa. The others were selected around the normal density (V=18 cm^3 mol^{-1}).

The calculated self-diffusion coefficient D is plotted against the inverse of temperature T in Fig. 3 by circles where pressure P is about 50 MPa. The experimental results at P=50 MPa are shown by the solid line.[35-39] The calculated D is in agreement with the observed one with respect to the temperature dependence. The

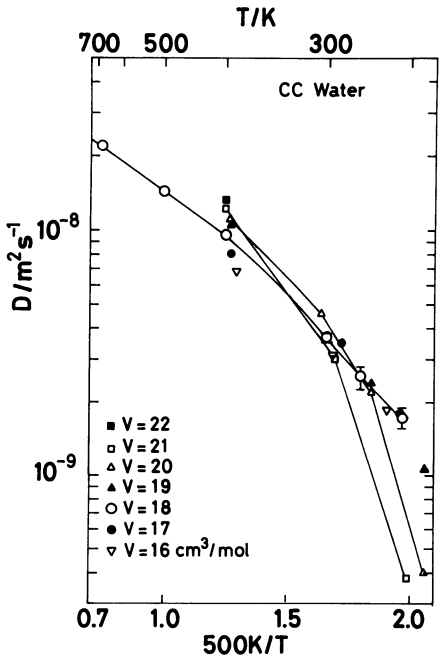

Fig. 4. The self-diffusion coefficient D is plotted against 500 K/T at several volumes.

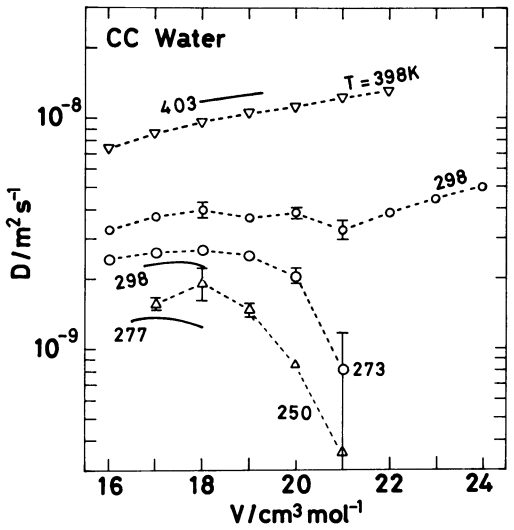

Fig. 5. The self-diffusion coefficient D is plotted against volume V at several temperatures. The experimental results are shown by the solid lines.[35-39]

calculations were repeated at different densities as seen in Fig. 4, where the setting temperatures were 260, 273, 298, 398, 500, and 700 K. As each average temperature was different from set temperature, the self-diffusion coefficients were obtained by interpolation as a function of temperature at each volume. The volume dependence of D obtained is shown in Fig. 5. The anomaly of the self-diffusion coefficient is semi-quantitatively reproduced as shown in Fig. 5. At lower temperatures, D has a maximum around volume V of

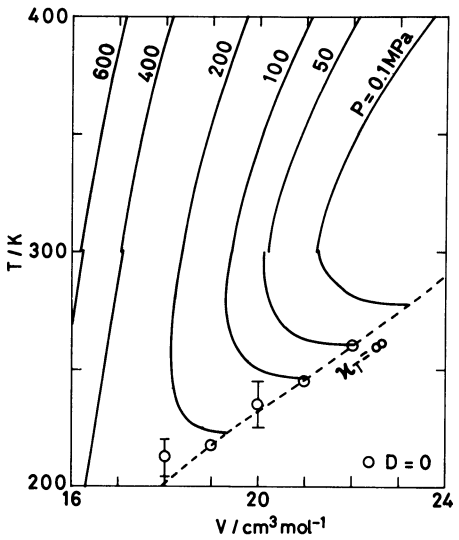

Fig. 6. The equation of state in the T-V plane. Above 300K the G-type EOS is used and below 300K the L-type EOS is shown.[4] The stability limit of the liquid phase is drawn by the dashed line.[4] The temperature where D is equal to zero at each volume is shown by circle.

18 $cm^3 mol^{-1}$ at a given temperature. Because the volume of the low density ice with CC potential is 11% larger than the observed one,[4] the volume with the maximum D at a given temperature varies correspondingly.

In this paper, the nonempirical calculation of the transport coefficients is intended; scaling of volume or adjusting have never been tried. The pressure effect on the self-diffusion coefficient of liquid water has been examined by a simple water-like model[1] and also by TIP4P model.[11]

When temperature is decreased, the self-diffusion coefficient D tends to approach to zero at a finite temperature under constant pressure as seen experimentally.[40] This temperature was discussed with the anomaly of the thermodynamic and transport properties of supercooled liquid water.[40-42] In the previous paper this temperature was assigned to the stability limit of liquid phase.[4]

Now we are going to see the relation between the stability limit of the liquid phase and the temperature of zero diffusion coefficient in this calculation.[43] We can get the temperature of zero D in the condition of fixed density as shown in Fig. 4. We used linear extrapolation for the D vs. T plot. The result is shown in Fig. 6. The circle means the temperature where D is equal to zero and the dotted line is the stability limit of the liquid phase obtained by the L-type equation of state.[4] We see that the zero D points are almost on the stability limit within the error bar. This means that the present calculations on the self-diffusion coefficient are consistent with the static properties obtained before.[4]

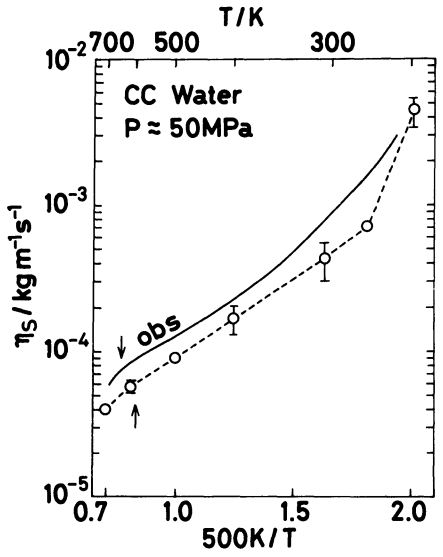

Fig. 7. The shear viscosity η_s is plotted against 500 K/T, where pressure is about 50 MPa. The experimental results at P=50 MPa are shown by the solid line.[44-50] An arrow indicates the critical temperature.

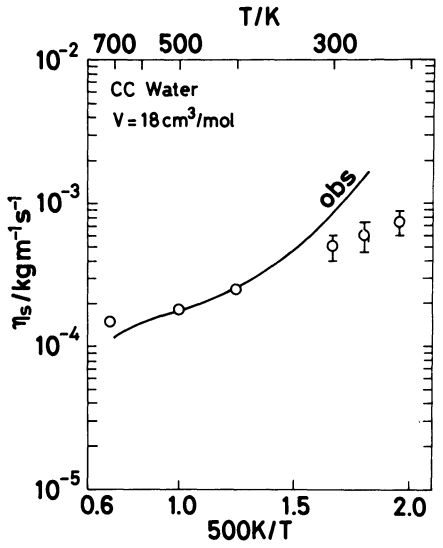

Fig. 8. The shear viscosity η_s is plotted against 500 K/T, where volume is 18 cm^3 mol^{-1}. The experimental results at V=18 cm^3 mol^{-1} are shown by the solid line.[44-50]

The shear viscosity η_s is plotted against the inverse of temperature in Fig. 7, where pressure P is about 50 MPa, and in Fig. 8 with the condition of the normal density (V=18 cm^3 mol^{-1}). The experimental results at P of 50 MPa are shown by solid line.[40-50] As regards the temperature dependence in Fig. 7, the obtained shear viscosity is in agreement with the observed one. Under the condition of normal density (Fig. 8), the calculated shear viscosity is a little smaller than the experimental results below room temperature. This can be understood qualitatively by the facts that the

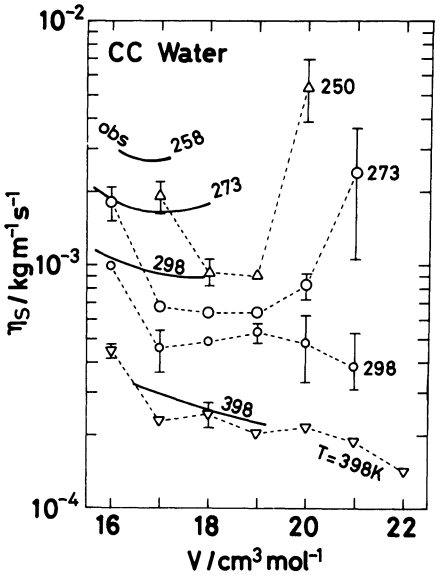

Fig. 9. The shear viscosity η_s is plotted against volume at several temperatures. The experimental reults are shown by the solid lines.[44-50]

shear viscosity of real liquid water at low temperatures has a minimum around P of 2×10^2 MPa as a function of pressure[7] and that the pressure is 2×10^2 MPa at room temperature by the present model.[4]

The volume dependence of η_s at several temperatures is shown in Fig. 9. This was obtained by interpolation as in the case of D. We see that the calculated shear viscosity has a peculiar volume dependence at low temperatures as observed in real water.[40-50] This property is shown much more clearly by the present simulation than in real water because our calculation includes the supercooled and/or minus pressure region. At a given temperature below room temperature, the volume of minimum viscosity is 18.5±0.5 cm^3 mol^{-1}, which is different a little from the observed one (around 17 cm^3 mol^{-1}). This comes from the reason that the length of hydrogen bond of the CC potential is larger than the observed one (see Table IV of Ref. 4).

The bulk viscosity η_B at normal density is plotted against the inverse of temperature in Fig. 10. The order of magnitude of the calculated values around room temperature is in agreement with the observed one.[51-53] As the bulk viscosity η_B is usually discussed by the ratio η_B/η_s, this quantity is plotted as a function of temperature in Fig. 11, where pressure is about 50 MPa for the calculation and the experimental results were obtained under normal pressure. Because of the large fluctuation of the virial term, the bulk viscosity at low temperatures was difficult to calculate in our case. The ratio η_B/η_s was larger than 1 below 500 K in accordance with the observed results.[51-53] The present calculation predicts that this quantity is less than 1 at higher temperatures, around or above the

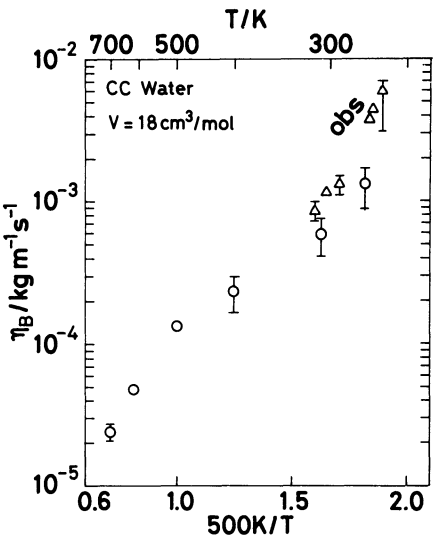

Fig. 10. The bulk viscosity η_B is plotted against 500 K/T, where volume is 18 cm^3 mol^{-1}. The experimental results are shown by the triangles.[51-53]

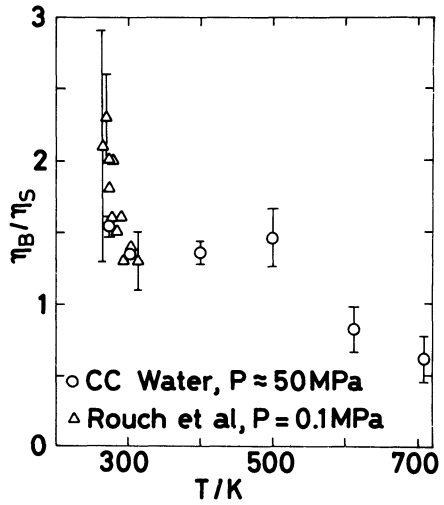

Fig. 11. The ratio η_B/η_S is plotted against temperature, where pressure is about 50 MPa for the calculation. The triangles show the experimental results[51-53] under normal pressure.

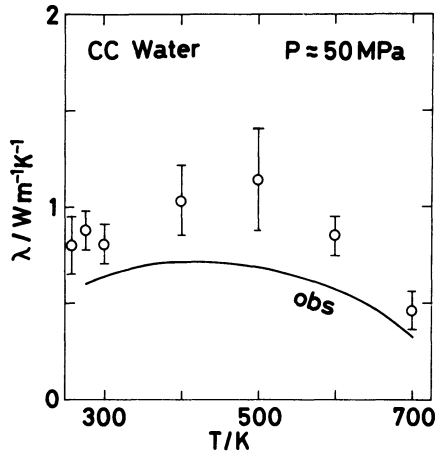

Fig. 12. The thermal conductivity λ is plotted against temperature, where pressure P is about 50 MPa. The experimental results at P=50 MPa are shown by the solid line.[50,54,55]

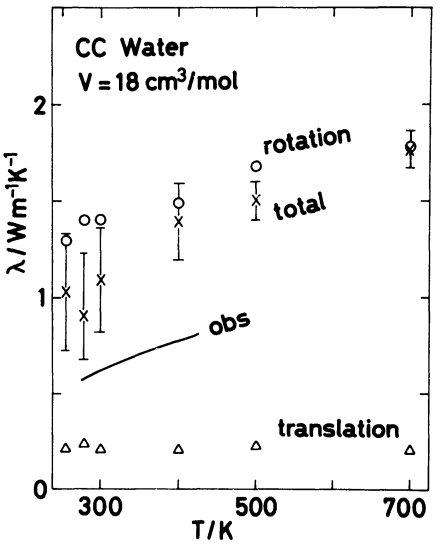

Fig. 13. The thermal conductivity λ is plotted against temperature, where volume is 18 cm^3 mol^{-1}. The cross means the total conductivity. The contribution from rotation and translation are plotted by circle and triangle respectively. The experimental results at V=18 cm^3 mol^{-1} are shown by the solid line.[50]

critical temperature (603 K for CC water).

The calculated thermal conductivity λ is shown as a function of temperature by open circle in Fig. 12, where pressure is about 50 MPa. We see that the present result is in agreement with the observed one at P of 50 MPa shown by the solid curve.[50,54,55] The thermal conductivity decreases as temperature increases above 500 K, because the density decreases abruptly around the critical temperature. So the essential point of anomaly in the thermal conductivity of liquid water is its increasing property with temperature at constant density. For this reason the thermal conductivity is plotted against temperature under the condition of normal density (V=18 cm^3 mol^{-1}) in Fig. 13. The cross indicates the calculated thermal conductivity at normal density, which is to be compared with the observed result shown by the solid curve at the same density.[50] The order of magnitude and the temperature dependence of the present values are in agreement with experiments.

In order to see the origin of this anomaly, partitioning of the thermal conductivity is tried as follows. The heat current $S(t)$ was divided into three parts, which are tentatively called translational, rotational, and molecular Hamiltonian part;

$$S(t) = S_{TRANS}(t) + S_{ROT}(t) + S_{MH}(t), \quad (10)$$

$$S_{\mathrm{TRANS}}(t) = \sum_{i=1}^{N}\{\frac{\mathrm{d}K_{\mathrm{TRANS}}(i)}{\mathrm{d}t} + \frac{1}{2}\sum_{i=1}^{N}(\frac{\partial U_{ij}}{\partial x_j}\frac{\mathrm{d}x_j}{\mathrm{d}t} + \frac{\partial U_{ij}}{\partial y_j}\frac{\mathrm{d}y_j}{\mathrm{d}t} + \frac{\partial U_{ij}}{\partial z_j}\frac{\mathrm{d}z_j}{\mathrm{d}t})\}r_i, \quad (11)$$

$$S_{\mathrm{ROT}}(t) = \sum_{i=1}^{N}\{\frac{\mathrm{d}K_{\mathrm{ROT}}(i)}{\mathrm{d}t} + \frac{1}{2}\sum_{i=1}^{N}(\frac{\partial U_{ij}}{\partial \omega_{1j}}\frac{\mathrm{d}\omega_{1j}}{\mathrm{d}t} + \frac{\partial U_{ij}}{\partial \omega_{2j}}\frac{\mathrm{d}\omega_{2j}}{\mathrm{d}t} + \frac{\partial U_{ij}}{\partial \omega_{3j}}\frac{\mathrm{d}\omega_{3j}}{\mathrm{d}t})\}r_i, \quad (12)$$

and

$$S_{\mathrm{MH}}(t) = \sum_{i=1}^{N} H_i \frac{\mathrm{d}r_i}{\mathrm{d}t} \quad (13)$$

where ω is the Euler angle. The total heat current was calculated by means of numerical differentiation as Eq. 7. The first and third terms of Eq. 10 were obtained at each MD step by Eqs. 11 and 13,[17] and the second term was indirectly calculated from other terms.

It was found that the contribution from molecular Hamiltonian part is negligible. The contributions from $S_{\mathrm{TRANS}}(t)$ and $S_{\mathrm{ROT}}(t)$ are shown as a function of temperature at normal density in Fig. 13. Although the contribution from the cross term of $S_{\mathrm{TRANS}}(t)$ and $S_{\mathrm{ROT}}(t)$ is not shown, we can estimate it graphically from the rest in Fig. 13. The main part is the contribution from the rotational one shown by circles. This part increases as temperature increases. On the other hand, the contribution from the translation part $S_{\mathrm{TRANS}}(t)$ is almost constant as a function of temperature and the magnitude is much less than that of the rotational one. The strong anisotropic interaction seems to be responsible to the rotational part.

Here we are going to understand the temperature dependence of the thermal conductivity in terms of the time correlation functions. For this purpose, we define the time correlation function as follows:

$$f_\lambda(t) = \langle \boldsymbol{S}(t)\cdot\boldsymbol{S}(0)\rangle. \quad (14)$$

The time correlation functions (translational and rotational parts) are shown in Figs. 14 and 15, respectively. The normal temperature case and the high temperature one are compared at normal density. As temperature increases, the correlation function of the rotational part changes more than that of the translational one at normal density as seen in Figs. 14 and 15.

For quantitative discussion on the temperature dependence, the time integral of the normalized correlation function is shown in Table 2. It is found that the time integral changes only a little with temperature under the condition of normal density (V=18 cm^3 mol^{-1}). However, not only the time integral but also the normalization constant $\langle \boldsymbol{S}(0)^2\rangle$

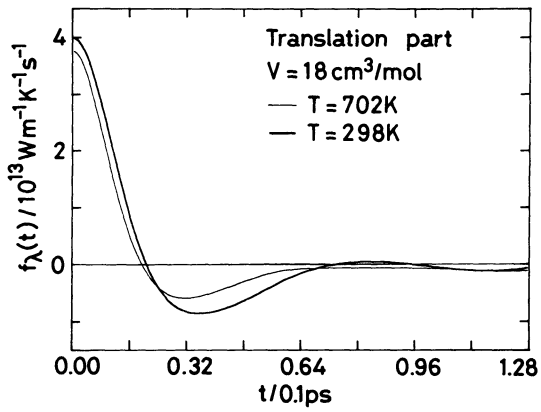

Fig. 14. The time correlation function related to the thermal conductivity, translational part.

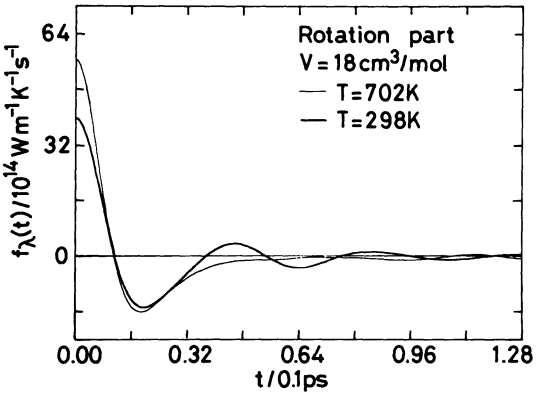

Fig. 15. The time correlation function related to the thermal conductivity, rotational part.

depends on temperature. These are summarized in Table 2 (cf. Eq. 6). From this table, it is seen that the increase of the factor $\langle \boldsymbol{S}(0)^2\rangle/T^2$ of the rotational part as a function of temperature is the main cause for the anomaly in the temperature dependence of the thermal conductivity of liquid water. The excitation of rotational motion is responsible to the increase of this factor.

In this paragraph we will try to compare liquid water with a simple liquid by the correlation function related to thermal conductivity. The heat current autocorrelation function in Lennard-Jones liquid does not have any clear oscillatory character.[27] On the other hand, the translational part of the correlation function of liquid water oscillates clearly as shown in Fig. 14. The Fourier transform has a maximum around 70 ps^{-1} although the figure is not shown. The above difference between simple liquid and liquid water comes from rotational motion and anisotropic interaction. The anisotropic potential energy has high frequency component because of the rotational motion in liquid water. This effect will be discussed in the next section.

Table 2. Rotational and Translational Parts of Thermal Conductivity, V=18 cm^3 mol^{-1}

			T/K	
			298	702
Rotational	$\int_0^\infty \frac{<S(t)\cdot S(0)>}{<S(0)^2>} dt$	10^{-15} s	0.36	0.32
	$\frac{<S(0)^2>}{3\kappa_B T^2 V}$	10^{15} W mK^{-1} s^{-1}	3.9	5.6
	λ_{ROT}	W mK^{-1}	1.4	1.8
Translational	$\int_0^\infty \frac{<S(t)\cdot S(0)>}{<S(0)^2>} dt$	10^{-15} s	5.0	5.5
	$\frac{<S(0)^2>}{3\kappa_B T^2 V}$	10^{13} W mK^{-1} s^{-1}	4.0	3.7
	λ_{TRANS}	W mK^{-1}	0.20	0.20

Time Correlation Functions

As the CC model[5] is not so different from MCY potential,[18] the kinetic properties of CC water are similar to those of MCY water.[9] Qualitatively these properties are not so different from those of BNS water.[8] The frequency spectrum of the velocity autocorrelation function has peaks at 8 and 30 ps^{-1}. The frequency spectra of angular velocity autocorrelations have peaks at 76, 120, and 100 ps^{-1} for α=1, 2, and 3 components in the Rahman and Stillinger's notation.[8]

The normalized correlation function related to shear viscosity is drawn in Fig. 16 at normal conditions (at room temperature and V of 18 cm^3 mol^{-1}). Its Fourier transform is compared with that at a higher temperature (T=702 K) in Fig. 17. We see two characteristic frequencies 40 and 160 ps^{-1} in Fig. 17 at room temperature. At high temperature (T=702 K), these peaks shift to lower frequencies. The oscillation of the time correlation function related to shear viscosity is not intrinsic in Lennard-Jones liquid.[26] However oscillation is clear in liquid water. Since there is strong anisotropic interaction in liquid water, the rotation-translation coupling can cause such an oscillatory behavior as discussed below in the paragraph on the thermal conductivity.

The bulk viscosity was obtained by the time integration of time correlation functions as shown in Fig. 18. In this case, an exponential decay is clear in short term. It is also possible to analyze the second part as another exponential decay as shown by the dotted line. The Fourier transform is given in Fig. 19, where the abscissa is in logarithmic scale. The zero-frequency is the main component at room temperature and a peak is seen around 6 ps^{-1} at T of 702 K in Fig. 19.

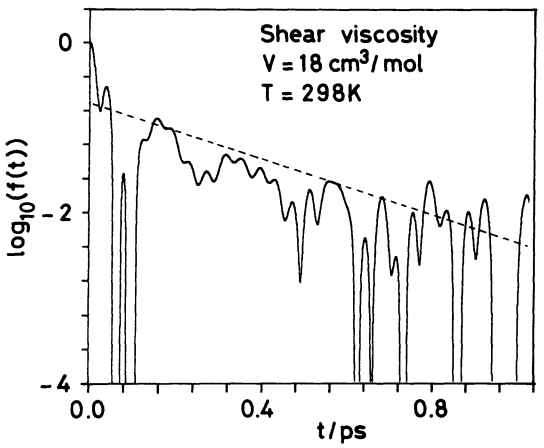

Fig. 16. The normalized time correlation function related to the shear viscosity. A decay character of the envelope is analyzed as shown by the dotted line.

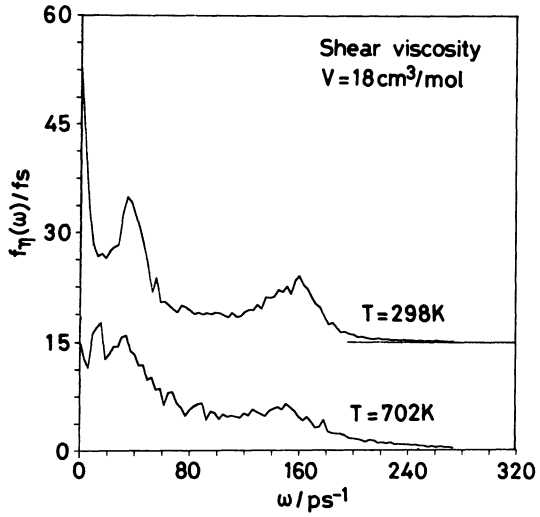

Fig. 17. The Fourier spectrum of the normalized time correlation function related to the shear viscosity.

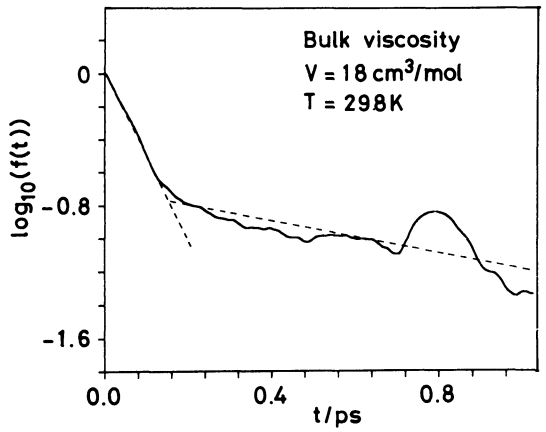

Fig. 18. The normalized time correlation function related to the bulk viscosity.

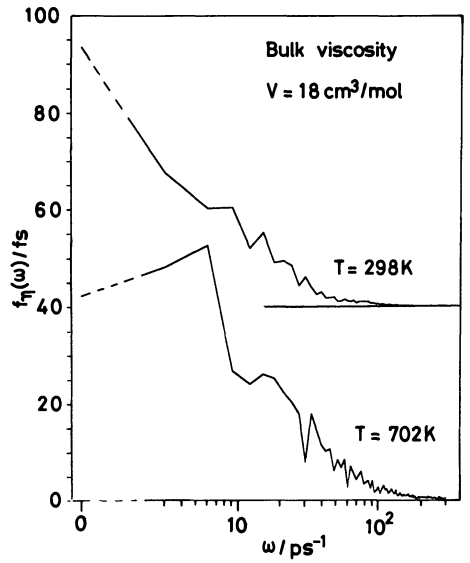

Fig. 19. The Fourier spectrum of the normalized time correlation function related to the bulk viscosity.

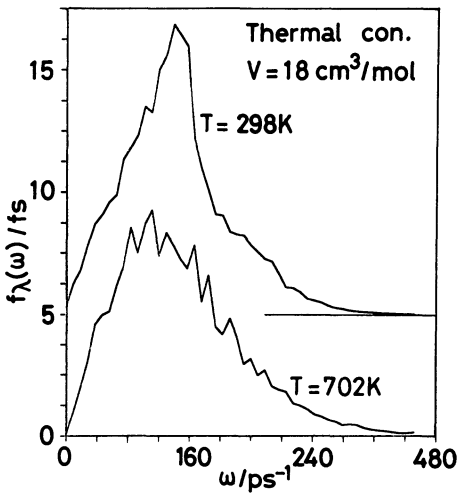

Fig. 20. The Fourier spectrum of the normalized time correlation function related to the thermal conductivity.

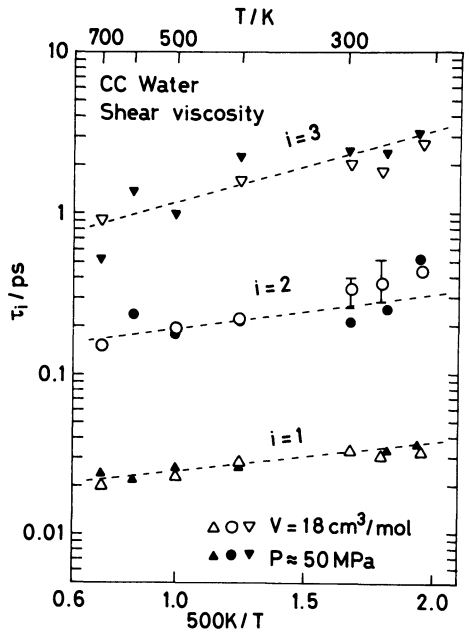

Fig. 21. The decay constant τ_i in Eq. 15, shear viscosity.

The decay character of the time correlation function related to bulk viscosity shown in Fig. 18 is qualitatively similar to that of Lennard-Jones liquid[28] in contrast with the case of shear viscosity.

Because the rotational part is main, the time correlation function related to thermal conductivity is not so different from that given in Fig. 15. The Fourier transform of the total correlation function related to thermal conductivity is plotted in Fig. 20. An oscillatory character is very clear. It is interesting to see that the characteristic frequency at about 140 ps^{-1} in thermal conductivity is close to the frequency seen in shear viscosity. The translational motion coupled with rotational one may have this frequency.

The long tails of the normalized time correlation functions are analyzed by the time averaged correlation functions which are averaged over a period of 0.144 ps, because the time correlation function oscillates with high frequency. The decay character of the time averaged correlation function was obtained by its envelope at long term. The short term was, however, analyzed by the original time correlation function. The following function was assumed (see Fig. 18):

$$f(t) = C_1 \exp(-t/\tau_1)\ t<0.1\ \mathrm{ps}(\eta_s),\ t<0.2\ \mathrm{ps}(\eta_B),$$

$$f(t) = C_2 \exp(-t/\tau_2)\ 0.1\ \mathrm{ps}<t<0.5\ \mathrm{ps}(\eta_s),\ 0.2\ \mathrm{ps}<t(\eta_B),$$

and

$$f(t) = C_3 \exp(-t/\tau_3)\ 0.5\ \mathrm{ps}<t<4\ \mathrm{ps}(\eta_s). \quad (15)$$

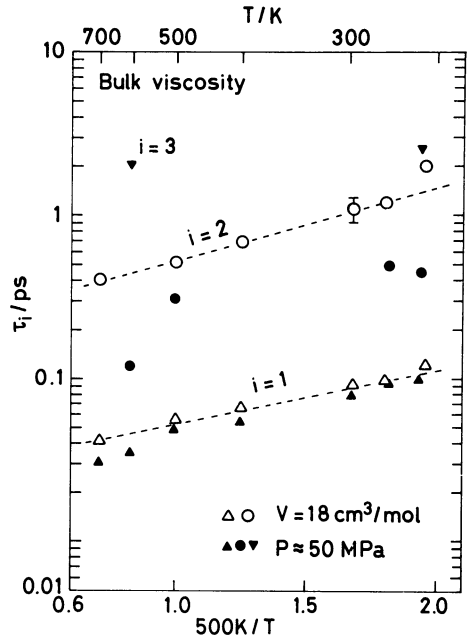

Fig. 22. The decay constant τ_i in Eq. 15, bulk viscosity.

The results on the decay constants τ_i are summarized in Figs. 21 and 22 for shear and bulk viscosity. It was difficult to perform such analysis on the time correlation function related to thermal conductivity, because of too high frequency components. These figures show that there are several decay constants and that the order of magnitude of them are 0.01, 0.1, and 1 ps. Wide distribution of decay constants means that there are so many time constants in the molecular motion in liquid water.

It is shown in this paper that anomalous behavior of the transport coefficients of liquid water can be reproduced nonempirically on a qualitative level. Some microscopic characteristics were revealed by the time correlation function related to the transport coefficients. The dynamical structure of liquid water will be studied in the next step.

The author would like to thank Prof. Nobuhiro Go and Mr. Mitsuhiro Matsumoto for valuable discussions. He also thanks Dr. D. Fincham, Queen Mary College, and Dr. W. Smith, Science and Research Council, Daresbury Laboratory, UK for their program MDMPOL as the basis of the present program. This work has been supported in part by a Grant-in-Aid for Scientific Research (Nos. 62103012, 62124039, and 63430023) from the Ministry of Education, Science and Culture. The author thanks the Computer Center of the Institute for Molecular Science for the use of HITAC M-680H and S-820/80 computers. The computation was also done by FACOM VP-400E and M-780 computers at Kyoto University Data Processing Center.

References

1) Y. Kataoka, *Bull. Chem. Soc. Jpn.*, **59**, 1425 (1986).
2) K. Okazaki, S. Nosé, Y. Kataoka, and T. Yamamoto, *J. Chem. Phys.*, **75**, 5864 (1981).
3) Y. Kataoka, *Bull. Chem. Soc. Jpn.*, **57**, 1522 (1984).
4) Y. Kataoka, *J. Chem. Phys.*, **87**, 589 (1987).
5) V. Carravetta and E. Clementi, *J. Chem. Phys.*, **81**, 2646 (1984).
6) M. Matsumoto and Y. Kataoka, *J. Chem. Phys.*, **88**, 3233 (1988).
7) G. S. Kell, "Water, a Comprehensive Treatise," ed by F. Franks, Plenum, New York (1972), Vol. 1, p. 363.
8) A. Rahman and F. H. Stillinger, *J. Chem. Phys.*, **55**, 3336 (1971). F. H. Stillinger and A. Rahman, *J. Chem. Phys.*, **61**, 4973 (1974).
9) R. W. Impey, P. A. Madden, and I. R. McDonald, *Mol. Phys.*, **46**, 513 (1982).
10) G. Jancso, P. Bopp, and K. Heinzinger, *Chem. Phys.*, **85**, 377 (1984).
11) M. R. Reddy and M. Berkowitz, *J. Chem. Phys.*, **87**, 6682 (1987).
12) M. W. Evans, G. C. Lie, and E. Clementi, *J. Chem. Phys.*, **88**, 5157 (1988).
13) M. Wojcik and E. Clementi, *J. Chem. Phys.*, **85**, 6085 (1986).
14) As for more comprehensive references on MD of liquid water, see the review articles cited in Ref. 4 and the references cited in Ref. 4. See also: A. C. Belch and S. A. Rice, *J. Chem. Phys.*, **86**, 5676 (1987). M. W. Evans, G. C. Lie, and E. Clementi, *J. Chem. Phys.*, **87**, 6040 (1987). H. Tanaka and I. Ohmine, *J. Chem. Phys.*, **87**, 6128 (1987).
15) R. Zwanzig, *Ann. Rev. Phys. Chem.*, **16**, 67 (1965).
16) D. J. Evans and W. B. Streett, *Mol. Phys.*, **36**, 161 (1978).
17) R. Kubo, "Water and Steam, Their Properties and Current Industrial Applications", Proc. 9th Intern. Conf. on Prop. of Steam, held at München, 1979, Pergamon (1980), p. 303.
18) O. Matsuoka, E. Clementi, and M. Yoshimine, *J. Chem. Phys.*, **64**, 1351 (1976).
19) S. Nosé, *Mol. Phys.*, **52**, 255 (1984); S. Nosé, *J. Chem. Phys.*, **81**, 511 (1984).
20) H. C. Andersen, *J. Chem. Phys.*, **72**, 2384 (1980).
21) D. Levesque, L. Verlet, and J. Kürkijarvi, *Phys. Rev. A*, **7**, 1690 (1973).
22) W. T. Ashurst and W. G. Hoover, *Phys. Rev.*, **11**, 658 (1975).
23) J. Vermesse and D. Levesque, *Phys. Rev.*, **19**, 1801 (1979).
24) D. M. Heyes, *J. Chem. Soc., Faraday Trans. 2*, **79**, 1741 (1983).
25) D. Fincham and D. M. Heyes, *Chem. Phys.*, **78**, 425 (1983).
26) M. Schoen and C. Hoheisel, *Mol. Phys.*, **56**, 653 (1985).
27) R. Vogelsang, C. Hoheisel, and G. Ciccotti, *J. Chem. Phys.*, **86**, 6371 (1987).
28) C. Hoheisel, *J. Chem. Phys.*, **86**, 2328 (1987). C. Hoheisel, R. Vogelsang, and M. Schoen, *J. Chem. Phys.*, **87**, 7195 (1987).
29) D. Levesque and L. Verlet, *Mol. Phys.*, **61**, 143 (1987).

30) W. Smith and D. Fincham, CCP5 Newsletter, an informal letter freely available from Science & Research Council, Daresbury Laboratory, Warrington WA4, 4AD, England.
31) J. Kushick and B. J. Berne, "Statistical Mechanics, Part B: Time-Dependent Processes," ed by B. J. Berne, Plenum, New York (1967), p. 41.
32) M. Neumann, *J. Chem. Phys.*, **82**, 5663 (1985).
33) M. Neumann, *J. Chem. Phys.*, **85**, 1567 (1986).
34) J. Anderson, J. J. Ullo, and S. Yip, *J. Chem. Phys.*, **87**, 1726 (1987).
35) L. A. Woolf, *J. Chem. Soc., Faraday Trans. 1*, **71**, 784 (1975).
36) L. A. Woolf, *J. Chem. Soc., Faraday Trans. 1*, **72**, 1267 (1976).
37) D. J. Wilbur, T. DeFries, and J. Jonas, *J. Chem. Phys.*, **65**, 1783 (1976).
38) K. Krynicki, C. D. Green, and D. W. Sawyer, *Faraday Discuss. Chem. Soc.*, **66**, 199 (1978).
39) K. R. Harris and L. A. Woolf, *J. Chem. Soc., Faraday Trans. 1*, **76**, 377 (1980).
40) R. J. Speedy and C. A. Angell, *J. Chem. Phys.*, **65**, 851 (1976).
41) C. A. Angell, "Water, a Comprehensive Treatise," ed by F. Franks, Plenum, New York (1981), Vol. 7, p. 1.
42) R. J. Speedy, *J. Phys. Chem.*, **86**, 982 (1982).
43) R. J. Speedy showed that the self-diffusion coefficient of the stretched model water tends to zero at low temperatures, "Abstracts of Lectures and Posters of Eighth International Symposium on Solute–Solute–Solvent Interactions," (1987), ed by J. Barthel and G. Schmeer, p. 29.
44) P. W. Brigeman, *Proc. Am. Acad. Arts Sci.*, **61**, 57 (1926).
45) K. E. Bett and J. B. Cappi, *Nature (London)*, **207**, 620 (1965).
46) E. M. Stanley and R. C. Batten, *J. Phys. Chem.*, **73**, 1187 (1969) and the references cited herein.
47) J. Kestin, H. E. Khalifa, H. Sookiazian, and W. A. Wakeham, *Ber. Bunsenges. Phys. Chem.*, **82**, 180 (1978).
48) T. DeFries and J. Jonas, *J. Chem. Phys.*, **66**, 896 (1977).
49) T. DeFries and J. Jonas, *J. Chem. Phys.*, **66**, 5393 (1977).
50) J. Kestin, J. V. Sengers, B. Kamgar-Parsi, and J. M. H. Levelt Sengers, *J. Phys. Chem. Ref. Data*, **13**, 175 (1984).
51) J. Rouch, C. C. Lai, and S.-H. Chen, *J. Chem. Phys.*, **65**, 4016 (1976).
52) J. Rouch and C. C. Lai and S.-H. Chen, *J. Chem. Phys.*, **66**, 5031 (1977).
53) J. Teixeira and J. Leblond, *J. de Phys.*, **39**, L83 (1978).
54) E. McLaughlin, *Chem. Eng.*, **64**, 389 (1964).
55) J. Yata, T. Minamiyama, T. Kim, and H. Murai, "Water and Steam, Their Properties and Current Industrial Applications," Proc. 9th Intern. Conf. on Prop. of Steam, held at München, 1979, Pergamon (1980), p. 431.